EXPERIMENTS WITH THE SEMI-LAGRANGIAN VERSION OF THE BMRC GLOBAL SPECTRAL ATMOSPHERIC MODEL

Michael Naughton and William Bourke
Bureau of Meteorology Research Centre, Melbourne, Australia

ABSTRACT

Two semi-Lagrangian advection schemes have been implemented in the BMRC global model — a standard Ritchie type U-V scheme and a new vorticity-divergence formulation. The new formulation is a three time level semi-implicit spectral application of the semi-Lagrangian method to the scalar advection equations for vorticity and divergence. The semi-Lagrangian formulations are described and some numerical results with the two versions are presented.

1. Introduction

Following the work of Ritchie and co-workers (Ritchie 1988, 1991, Ritchie et al. 1995) we have implemented the three time level semi-implicit semi-Lagrangian advection scheme in the BMRC global spectral model (Bourke et al. 1977, Bourke 1988). Several of the standard refinements have been included in the model: (i) using the Taylor series tangent plane approximations away from the poles (Ritchie & Beaudoin 1994), (ii) spatial averaging between the backward and forward time level trajectory points for terms evaluated at the intermediate time level (Tanguay et al. 1992), (iii) "quasi-cubic" mixed cubic-linear interpolation formulae (Ritchie et al. 1995).

This version of the BMRC global spectral model contains several other options: (i) reduced grid (Hortal & Simmons 1991, Courtier & Naughton 1994), (ii) option of using different resolution grids in the different transform loops for dynamics, physics, data analysis, (iii) choice of triangular or rhomboidal truncation, (iv) dynamic memory allocation to enable run-time setting of resolution dimensions.

A new variant of the spectral semi-Lagrangian method has also been developed which applies the semi-Lagrangian technique to the scalar equations for vorticity and divergence.

2. U-V Semi-Lagrangian Formulation

Since our U-V semi-Lagrangian implementation follows Ritchie's formulation in most respects, only a brief description is given of the scheme to highlight the differences in our implementation.

The semi-Lagrangian scheme has been implemented within the framework of the existing BMRC spectral model, which is an Eulerian vorticity-divergence semi-implicit model with two transform loops for dynamics and physical processes.

The horizontal momentum equations are

$$\frac{d\mathbf{u}}{dt} + f\mathbf{k} \times \mathbf{u} + \nabla\phi_v + R_v T \nabla(\ln p_s) = F_{\mathbf{u}} \tag{2.1}$$

which can be expressed in terms of the wind images (U, V), where $U = u\cos\theta/a$, $V = v\cos\theta/a$, as

$$\frac{\partial U}{\partial t} + A(U,V,U) + \dot{\sigma}\frac{\partial U}{\partial \sigma} - fV + \frac{1}{a^2}\left(\frac{\partial \phi_v}{\partial \lambda} + RT_v\frac{\partial}{\partial \lambda}(\ln p_s)\right) = F_U \tag{2.2}$$

$$\frac{\partial V}{\partial t} + A(U,V,V) + 2\sin\theta E + \dot{\sigma}\frac{\partial V}{\partial \sigma} + fU + \frac{1}{a^2}\left(\cos\theta\frac{\partial \phi_v}{\partial \theta} + RT_v\cos\theta\frac{\partial}{\partial \theta}(\ln p_s)\right) = F_V \tag{2.3}$$

$$E = \frac{(U^2 + V^2)}{2\cos^2\theta} \tag{2.4}$$

The semi-implicit time stepping algorithm differs from the scheme of Ritchie (1991) in the linearization of the temperature equation. The temperature equation is

$$\frac{1}{T}\frac{dT}{dt} = \frac{R_v}{c_p}\frac{1}{p}\frac{dp}{dt}$$

or

$$\frac{dT}{dt} = \frac{R_v T}{c_{pv}}\frac{\omega}{p}$$

where $\omega = dp/dt$, $\sigma = p/p_s$,

$$\frac{\omega}{p} = \frac{\dot{\sigma}}{\sigma} - \frac{\partial \dot{\sigma}}{\partial \sigma} - \delta$$

which can be expressed in terms of δ, $\mathbf{u}$, $\ln p_s$ as

$$\frac{\omega}{p} = \left\{\int_1^0 \delta\, d\sigma' - \int_1^\sigma \delta\, d\sigma' + \left(\int_1^0 \mathbf{u}\, d\sigma' - \int_1^\sigma \mathbf{u}\, d\sigma' + \sigma\mathbf{u}\right).\nabla(\ln p_s)\right\}/\sigma$$

The moist gas constant and specific heat for moist air are given by the formulae

$$R_v \sim (1 + 0.61q)R_g$$

$$c_{pv} \sim (1 + 0.87q)c_p$$

where R_g, c_p are the constants for dry air, so, keeping only the linear term in q,

$$\left(\frac{R}{c_p}\right)_v = \frac{R_v}{c_{pv}} \sim \frac{R_g}{c_p}(1 - 0.26q)$$

The linear part of the divergence component of the temperature tendency is the term which is treated semi-implicitly

$$\frac{R_g\overline{T}(\sigma; t=0)}{c_p\sigma}\left(\int_1^0 \delta\, d\sigma' - \int_1^\sigma \delta\, d\sigma'\right)$$

since this term is linear in the divergence it can be handled conveniently in spectral space. The other terms which are calculated semi-implicitly are the $\nabla\phi$ and $R_g\overline{T}(\sigma; t=0)\nabla(\ln p_s)$ parts of the $\nabla\phi_v$ and $R_vT\nabla(\ln p_s)$ terms in the in the momentum equations and the $\int_0^1 \delta\, d\sigma'$ term in the surface pressure equation. The residual parts of these terms are calculated centred in time †.

The vertical discretization in sigma coordinates uses the same scheme as in the Eulerian model version (Bourke 1974) with some slightly different terms being needed for the vertical trajectory and vertical advection calculations; one of the the additional terms which is needed for the continuity equation is $\partial\dot{\sigma}/\partial\sigma$, given by

$$\frac{\partial\dot{\sigma}}{\partial\sigma} = -\left(\int_1^0 \delta(\sigma')d\sigma' + \delta\right) - \left(\int_1^0 \mathbf{u}(\sigma')d\sigma' + \mathbf{u}\right).\nabla(\ln p_s)$$

This is the vertical velocity term in the multilevel form of the continuity equation which vanishes in the vertically averaged continuity equation in the Eulerian model formulation, but not in the semi-Lagrangian equations. The semi-Lagrangian discretization of the continuity equation uses the two dimensional trajectory given by the horizontal components of the full trajectory used for the other equations; note that in the 3D and 3D-NIV schemes this will not be identical to calculating a separate two-dimensional trajectory, but the difference is assumed to be negligible (Ritchie et al. 1995).

One of the subtleties of the spectral semi-Lagrangian schemes involves the order of operations between spectral differentiation and grid point interpolation. In general these two operations do not commute and care is required to ensure that calculations are made in the correct order. One term which requires different treatment for this reason is the residual part of the geopotential in the divergence equation. In the vorticity-divergence Eulerian scheme this term is included in the divergence equation as $\nabla^2(\phi_v - \phi)$, in combination with the $\nabla^2 E$ term — the quantity $E + (\phi_v - \phi)$ is calculated in grid point space and transformed to spectral space where the ∇^2 operator is applied. Whilst the $\nabla^2 E$ term is not present in

† Actually, in the present implementation the $R_g\left(\overline{T}(\sigma,t) - \overline{T}(\sigma,t=0)\right)$ contribution is lagged in time; since it is calculated spectrally in the Eulerian code, it has been combined with other linear lagged terms calculated spectrally in the semi-Lagrangian version.

the semi-Lagrangian scheme the geopotential term must still be calculated. To calculate this term correctly in the U-V semi-Lagrangian form the horizontal derivatives of T and q are transformed to the grid, $\nabla(\phi_v - \phi)$ calculated and then interpolated to the departure points, transformed to spectral space and then the divergence calculated spectrally. If the Eulerian algorithm is naively translated to the semi-Lagrangian scheme by interpolating $(\phi_v - \phi)$ the result is different; The difference can readily be seen by observing that the resultant interpolated field is defined at the departure points, not on the model Gaussian grid, so the usual spectral transform and multiplication will not give the true Laplacian for this irregularly spaced grid. In practice, because this correction term is small the difference is not significant, but the correct calculation is nonethelesss clearly preferable. Note that this term is not present in the ECMWF model version which uses virtual temperature as the spectral variable (Ritchie et al. 1995).

More generally, any nonlinear terms involving horizontal differention must be calculated in advective form (instead of flux form) in the semi-Lagrangian scheme so that they can be available to be interpolated on the grid when they have been evaluated. The only correct way to treat nonlinear terms in flux form would be to add an extra transform to spectral space and back to grid point space, which would be more complicated and add an undesirable computational overhead.

Computational details — multitasking strategy

Both the Eulerian and semi-Lagrangian model version are multi-tasked for shared memory parallel vector computer architecture. The dynamics and physics multi-tasking is primarily over latitude except for the transform from Fourier coefficients to spherical harmonic coefficients where the accumulation over latitudes is multi-tasked over zonal wavenumber instead (Dent 1992, Bourke et al. 1995). The BMRC model is an "in-core" model, i.e. there is no use of "gridpoint workfiles" during the calculation to store temporary grid point and Fourier coefficient fields. In order to conserve space the primary dynamical fields are stored in spectral space and the Fourier and grid point representations are calculated and used one latitude at a time.

For the semi-Lagrangian scheme the latitude processing strategy must be modified because the the trajectory calculations and departure point interpolations require information from several neighbouring latitudes for the semi-Lagrangian calculations at each arrival point of the regular Gaussian grid. To accomplish this a cyclic band of latitudes is used (as in the ECMWF model) — the required calculations are split into two phases, the first to compute the information required for the interpolations and the second to perform the trajectory calculations and semi-Lagrangian interpolations. These two phases of the calculation are lagged such that the first leads the second by several latitudes, so that the neighbouring latitudes information is ready when it is needed. The cyclic grid buffer is used in such a way

that latitudes are overwritten when they are no longer needed for successive interpolations. For multi-tasking purposes the latitudes are grouped into bands such that a band of several latitudes is processed simultaneously to the point where the Fourier coefficients have been calculated for the spherical harmonic coefficients. At this point the multi-tasked calculations are synchronized and the contribution of this band of latitudes to the spectral coefficients is calculated. With this scheme the Fourier coefficient arrays can be reused for each band of latitudes, reducing the memory required to store them or the need to read and write them to disk. Likewise the use of a cyclic grid buffer for the interpolation step economizes on storage of grid field data. The size of the cyclic grid buffer is equal to the maximum width of the departure point interpolation stencil for a band of latitudes, which depends on the meridional Courant number (i.e. maximum meridional velocity times time step divided by meridional grid spacing) and number of processors.

3. Numerical Experiments with U-V Semi-Lagrangian Model

The period from 1–14 February 1995 has been used for comparing several versions of the BMRC model and assimilation system with the current R53_L19 operational system, including the semi-Lagrangian schemes, triangular versus rhomboidal truncation, reduced Gaussian grids, mass flux moisture, linear grid resolution for the data assimilation and OI moisture assimilation. The operational (Eulerian) model uses a 9 minute time step, although at this time of year the stability limit is closer to 12 minutes. Fourth order implicit horizontal diffusion is used with diffusion coefficient 7.5 $\times 10^{15}$ m^4 s^{-1}. The Eulerian model and assimilation has been run at T79_L19 and T106_L19 through the period, with little difference between the R53_L19, T79_L19 and T106_L19 forecasts and verification statistics (ref. Fig 1†) compared to the significant positive impact of the mass flux physics changes (ref. Fig 2). The lack of skill improvement in going to higher resolution (not shown) suggests that adjustment of some of the topography generation, diffusion coefficients, etc., or perhaps increasing the number of vertical levels may be needed for the increased resolution.

Semi-Lagrangian forecasts have been run at both T79_L19 (full period) and T106_L19 (individual cases) resolutions starting from initial conditions from the Eulerian assimilation cycles with time steps of 20 minutes and 9 minutes. As in the Eulerian case the T106 forecasts did not improve upon T79 and we have focussed mostly on the T79 resolution. In the midlatitudes the forecast skill of the semi-Lagrangian scheme is comparable to the Eulerian scheme, but in the tropics there is a distinct cold bias in both the MSLP and geopotential height fields (Fig 3, Fig 4).

† The T79_L19 system used for these experiments also contained an improved (OI) moisture assimilation scheme, which has some impact in the tropics.

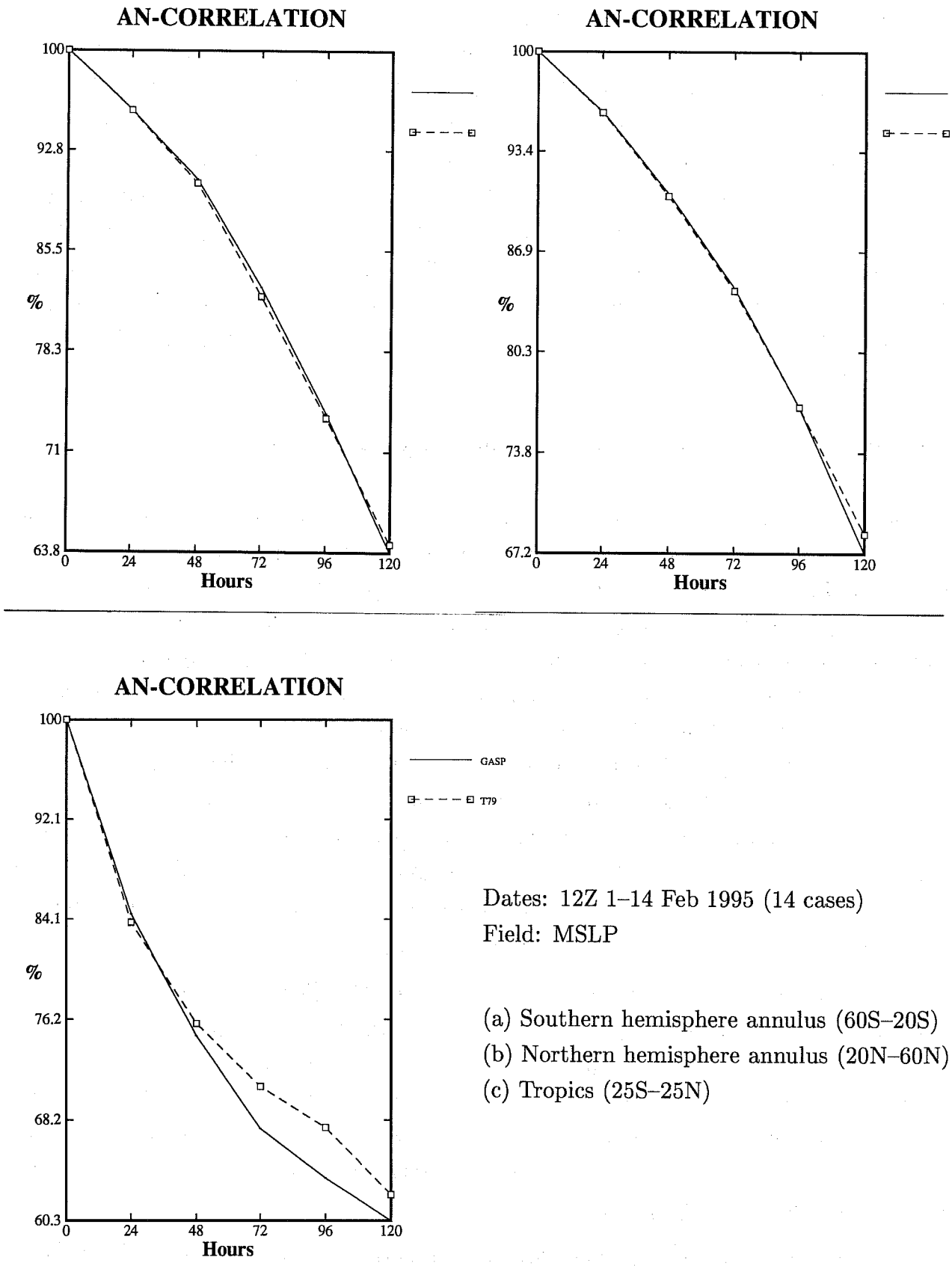

Dates: 12Z 1–14 Feb 1995 (14 cases)
Field: MSLP

(a) Southern hemisphere annulus (60S–20S)
(b) Northern hemisphere annulus (20N–60N)
(c) Tropics (25S–25N)

Fig 1. [**GASP**] Operational GASP R53_L19 vs [**T79**] T79_L19.

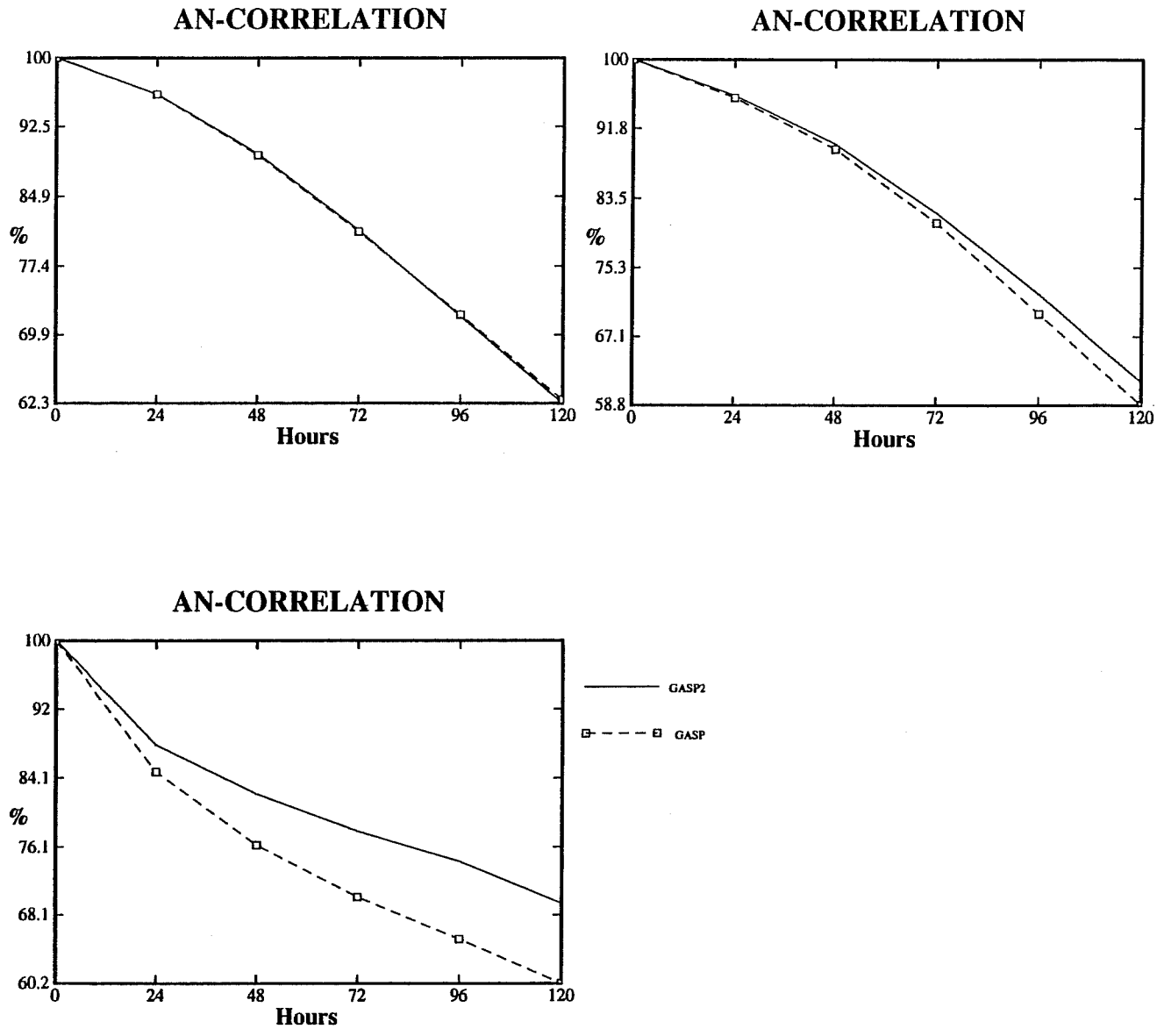

Dates: 00Z & 12Z 10 Sep – 28 Oct 1995 (82 cases)
Field: MSLP

(a) Southern hemisphere annulus (60S–20S)
(b) Northern hemisphere annulus (20N–60N)
(c) Tropics (25S–25N)

Fig 2. [**GASP2**] T79_L19 pre-operational trial (incl. massflux & interactive cloud optical properties & global ozone & OI moisture assimilation) vs [**GASP**] Operational GASP R53_L19.

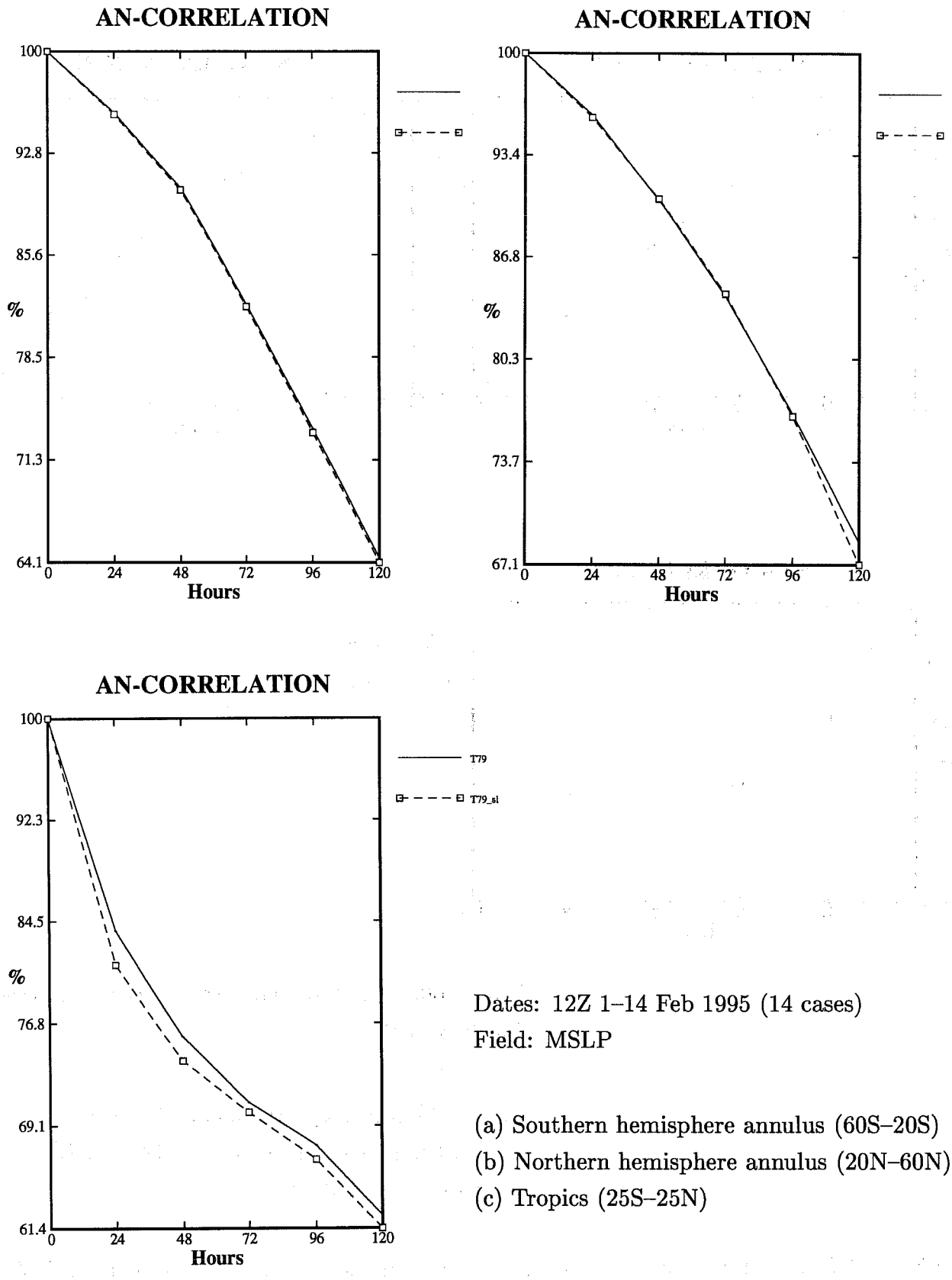

Dates: 12Z 1–14 Feb 1995 (14 cases)
Field: MSLP

(a) Southern hemisphere annulus (60S–20S)
(b) Northern hemisphere annulus (20N–60N)
(c) Tropics (25S–25N)

Fig 3. [**T79**] Eulerian T79 vs [**T79_sl**] Semi-Lagrangian T79.

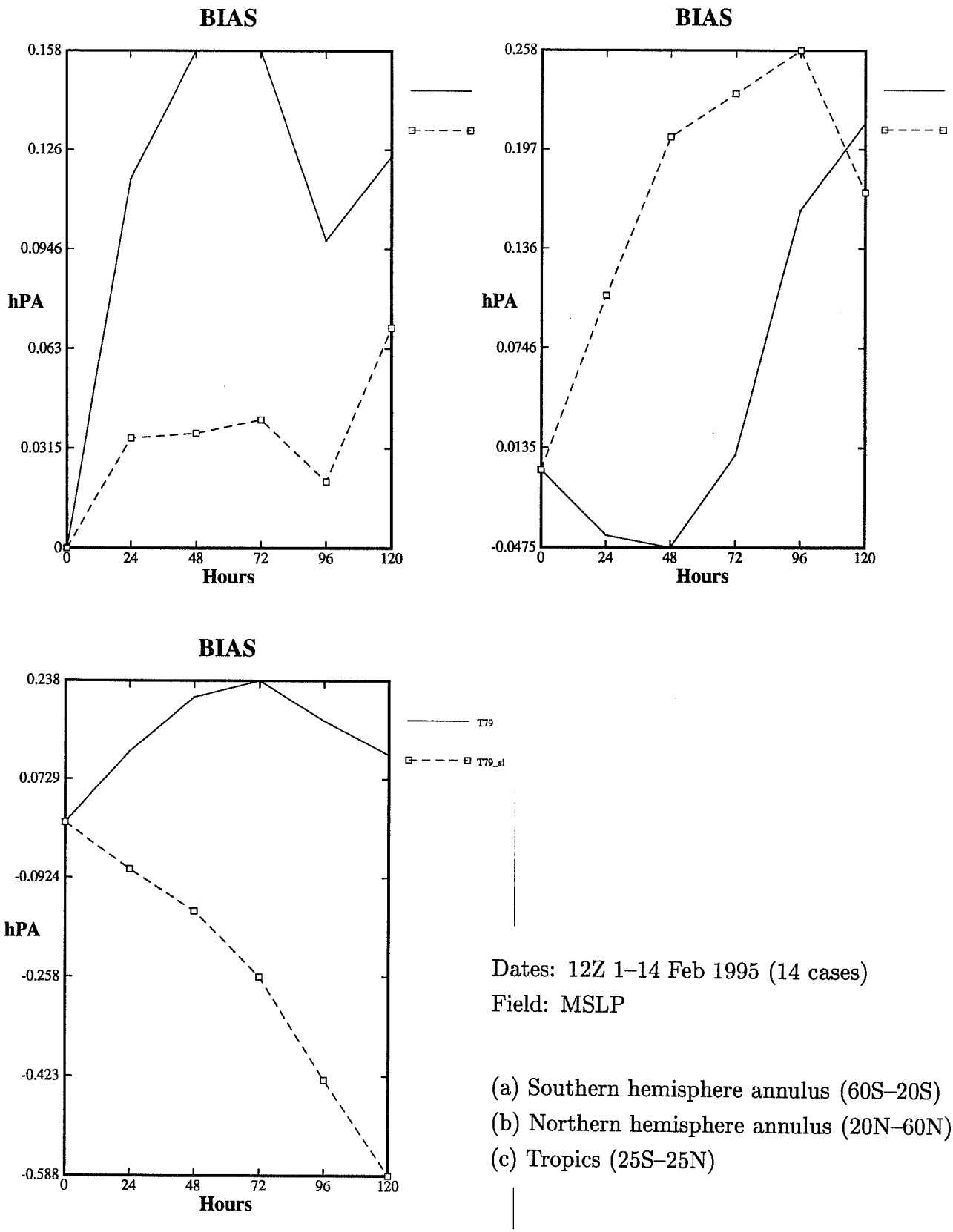

Dates: 12Z 1–14 Feb 1995 (14 cases)
Field: MSLP

(a) Southern hemisphere annulus (60S–20S)
(b) Northern hemisphere annulus (20N–60N)
(c) Tropics (25S–25N)

Fig 4. [**T79**] Eulerian T79 vs [**T79_sl**] Semi-Lagrangian T79.

The sensitivity to dynamics grid resolution while keeping physics grid resolution fixed has been examined at T79 and T106 by running with both coarser ("linear grid") and finer dynamics grids than the quadratic grid resolution: at T79 — 80×160 (linear), 120×240 (quadratic), 150×300 (fine grid), and at T106 — 108×216 (linear), 160×320 (quadratic), 200×400 (fine grid). The verifications show negligible difference between the quadratic and fine grid forecast skill, but the linear grid results are slightly less skillful. Of course, the linear grid is also cheaper than the quadratic grid, which would enable higher spectral resolution to be run at the same cost, but this comparison has not been attempted here.

4. Vorticity-Divergence Semi-Lagrangian Formulation

The vorticity-divergence semi-Lagrangian formulation applies semi-Lagrangian time integration to the evolution of the vertical component of vorticity and the horizontal divergence. Equations for these scalar quantities are obtained by taking the curl and divergence of the horizontal momentum equation, and expressing the advection terms as the advection of vorticity and divergence respectively plus additional terms which are evaluated and interpolated in the usual semi-Lagrangian manner. The nonlinear terms are most conveniently written in advective form so that they can be interpolated without need for derivatives to be taken after the nonlinear products are formed.

The equations for vorticity and divergence (ζ,δ) are obtained by taking the curl and divergence of the horizontal momentum equations (2.1). In terms of the (U,V) variables the horizontal curl and divergence operators are given by $\zeta=\mathbf{k}.\nabla\times\mathbf{u}=\alpha(V,-U)$, $\delta=\nabla.\mathbf{u}=\alpha(U,V)$. The following vector identities are also employed:

$$\alpha\Big(\ A(U,V,V)+2\sin\theta E\ ,\ -A(U,V,U)\ \Big)=A(U,V,\zeta)+\delta\zeta$$

$$\alpha\Big(\ A(U,V,U)\ ,\ A(U,V,V)+2\sin\theta E\ \Big)=A(U,V,\delta)+\delta^2-2J$$

where J is the Jacobian of the horizontal velocity field, which can be expressed as

$$J=\frac{1}{\cos^4\theta}\left\{\frac{\partial U}{\partial\lambda}\cos\theta\frac{\partial V}{\partial\theta}-\cos\theta\frac{\partial U}{\partial\theta}\frac{\partial V}{\partial\lambda}+\sin\theta\left(V\frac{\partial U}{\partial\lambda}-U\frac{\partial V}{\partial\lambda}\right)\right.$$
$$\left.-\sin\theta\left(U\cos\theta\frac{\partial U}{\partial\theta}+V\cos\theta\frac{\partial V}{\partial\theta}\right)-\frac{1+\sin^2\theta}{2}\left(U^2+V^2\right)\right\}$$

The vorticity and divergence equations become

$$\frac{\partial\zeta}{\partial t}+A(U,V,\zeta)+\dot\sigma\frac{\partial\zeta}{\partial\sigma}=$$
$$-\left\{\delta\zeta+\frac{1}{\cos^2\theta}\left[\frac{\partial\dot\sigma}{\partial\lambda}\frac{\partial V}{\partial\sigma}-\left(\cos\theta\frac{\partial\dot\sigma}{\partial\theta}\right)\frac{\partial U}{\partial\sigma}\right]+2\Omega(\delta\sin\theta+V)\right.$$
$$\left.+\frac{R}{a^2\cos^2\theta}\left[\left(\frac{\partial T_v}{\partial\lambda}\right)\left(\cos\theta\frac{\partial}{\partial\theta}(\ln p_s)\right)-\left(\cos\theta\frac{\partial T_v}{\partial\theta}\right)\left(\frac{\partial}{\partial\lambda}(\ln p_s)\right)\right]\right\}$$
$$+\alpha(F_V,-F_U) \tag{4.1}$$

$$\begin{aligned}\frac{\partial \delta}{\partial t} + A(U,V,\delta) + \dot{\sigma}\frac{\partial \delta}{\partial \sigma} = & \\ & - \left\{ \delta^2 - 2J + \frac{1}{\cos^2\theta}\left[\frac{\partial \dot{\sigma}}{\partial \lambda}\frac{\partial U}{\partial \sigma} + \left(\cos\theta \frac{\partial \dot{\sigma}}{\partial \theta}\right)\frac{\partial V}{\partial \sigma}\right] + 2\Omega(\zeta \sin\theta - U) \right. \\ & \quad + \nabla^2 \phi_v + \frac{RT_v}{a^2}\nabla^2(\ln p_s) \\ & \quad \left. + \frac{R}{a^2\cos^2\theta}\left[\frac{\partial T_v}{\partial \lambda}\frac{\partial}{\partial \lambda}(\ln p_s) + \left(\cos\theta \frac{\partial T_v}{\partial \theta}\right)\left(\cos\theta \frac{\partial}{\partial \theta}(\ln p_s)\right)\right]\right\} \\ & + \alpha(F_U, F_V)\end{aligned} \tag{4.2}$$

For simplicity, virtual temperature is approximated by the first term in the Taylor series as $T_v = T(1 + \epsilon q)$; the gradients of virtual temperature appearing above are evaluated using the product rule. The $\nabla^2 \phi_v$ term depends on $\nabla^2 T_v$ as

$$\begin{aligned}\nabla^2 \phi_v =& A\nabla^2 T_v \\ \nabla^2 T_v =& \left(\nabla^2 T\right)(1 + \epsilon q)) + T\left(\epsilon \nabla^2 q\right) \\ & + \frac{2\epsilon}{a^2\cos^2\theta}\left(\frac{\partial T}{\partial \lambda}\frac{\partial q}{\partial \lambda} + \left(\cos\theta \frac{\partial T}{\partial \theta}\right)\left(\cos\theta \frac{\partial q}{\partial \theta}\right)\right)\end{aligned}$$

where A is the vertical integration matrix for the hydrostatic equation.

The diagnostic relation for $\dot{\sigma}$ in terms of δ, U, V, $\ln(p_s)$ can be written as

$$\dot{\sigma} = I(\delta) + \frac{1}{\cos^2\theta}\left\{ I(U)\frac{\partial}{\partial \lambda}(\ln p_s) + I(V)\cos\theta \frac{\partial}{\partial \theta}(\ln p_s)\right\}$$

where

$$I(f) = I(f)(\sigma) = (1 - \sigma)\int_1^0 f(\sigma')d\sigma' - \int_1^\sigma f(\sigma')d\sigma'$$

This equation is differentiated horizontally in λ and θ to obtain expressions for calculating the terms involving $\dot{\sigma}$ on the right hand side of (4.1), (4.2):

$$\begin{aligned}\frac{\partial \dot{\sigma}}{\partial \lambda} = I\left(\frac{\partial \delta}{\partial \lambda}\right) + \frac{1}{\cos^2\theta}\left\{ \right. & I\left(\frac{\partial U}{\partial \lambda}\right)\frac{\partial}{\partial \lambda}(\ln p_s) + I(U)\frac{\partial^2}{\partial \lambda^2}(\ln p_s) \\ & \left. + I\left(\frac{\partial V}{\partial \lambda}\right)\cos\theta \frac{\partial}{\partial \theta}(\ln p_s) + I(V)\frac{\partial}{\partial \lambda}\left(\cos\theta \frac{\partial}{\partial \theta}(\ln p_s)\right)\right\}\end{aligned}$$

$$\begin{aligned}\cos\theta \frac{\partial \dot{\sigma}}{\partial \theta} = & I\left(\cos\theta \frac{\partial \delta}{\partial \theta}\right) \\ & + \frac{1}{\cos^2\theta}\left\{ \right. I\left(\cos\theta \frac{\partial U}{\partial \theta}\right)\frac{\partial}{\partial \lambda}\ln p_s + I(U)\cos\theta \frac{\partial}{\partial \theta}\left(\frac{\partial}{\partial \lambda}\ln p_s\right) \\ & \quad \left. + I\left(\cos\theta \frac{\partial V}{\partial \theta}\right)\cos\theta \frac{\partial}{\partial \theta}(\ln p_s) + I(V)\cos\theta \frac{\partial}{\partial \theta}\left(\cos\theta \frac{\partial}{\partial \theta}(\ln p_s)\right)\right\} \\ & + \frac{2\sin\theta}{\cos^2\theta}\left\{ I(U)\frac{\partial}{\partial \lambda}(\ln p_s) + I(V)\cos\theta \frac{\partial}{\partial \theta}(\ln p_s)\right\}\end{aligned}$$

In comparison with the (U, V) semi-Lagrangian formulation the extra nonlinear terms on the right hand side require additional grid point calculations and Legendre and Fourier transforms. Relative to the scheme described in Ritchie et al. (1995) four multilevel and one single level extra Legendre tranforms are needed if T is used as the spectral temperature variable, namely ζ, $cos\theta\partial\delta/\partial\theta$, $\nabla^2 T$, $\nabla^2 q$, $\nabla^2(\ln p_s)$, reducing to two additional multilevel transforms if virtual temperature is used as the spectral variable, since the ∇^2 terms are not needed in that case.

5. Numerical experiments with vorticity-divergence semi-Lagrangian model

Results from the vorticity-divergence semi-Lagrangian model are only preliminary at this stage as the model has only recently been written and is still in the process of being tested. In order to validate the coding of the model an "advective form vorticity-divergence Eulerian" option has been written, much in the same way as a U-V Eulerian model was developed as a preliminary step to the development of Ritchie's U-V semi-Lagrangian models. The terms $A(U, V, \zeta)$ and $A(U, V, \delta)$ in (4.1), (4.2) only require the gradient of vorticity on the grid in addition to fields already available, but this is readily calculated. The spectral coefficients of the Q terms calculated at $t = 0$ from the advective vorticity-divergence Eulerian form have been compared with the vorticity-divergence flux form and the U-V Eulerian form, with all three agreeing to a high degree of precision — in excess of 7 digits for a calculation using a uniform quadratic dynamics grid. This level of agreement is as expected since the dynamics terms contain at most quadratic nonlinearities so there are no truncation error differences only different roundoff errors between the different calculations. This agreement in the calculation of the Eulerian advection terms is sufficient to validate that the advective vorticity-divergence Eulerian formulation is equivalent to the other forms.

Tests with the vorticity-divergence semi-Lagrangian model have been less satisfactory, with two significant problems arising: a restrictive time step numerical stability limit and significantly larger and unacceptable errors compared with the Eulerian and U-V SL models. The numerical stability limit is intermediate between the U-V SL and Eulerian models, but much closer to the latter. The U-V SL model has been mostly run with a 20 min time step; a 30 min time step is still stable, but the forecast skill is significantly poorer and the fields are quite noisy in the tropics. For the 1 February case the Eulerian model with a 20 min time step becomes unstable almost immediately with wind speeds in excess of 200 m s^{-}1 being generated in less than 6 hours. The V-D SL model with a 20 min time step crashes after about 48 hours. With the time step reduced to 15 min or 12 min the V-D SL model ran to 5 days on the 1 February case, but failed on several of the other cases in the 1–14 Feb period. Finally the time step was reduced to 9 min producing satisfactory integrations for all cases.

Charts of the V-D SL model 5 day forecast from 1 February show that the main features of the flow are consistent with the other models (Fig 5), which demonstrates that the scheme is correctly solving the equations. However the forecast verification statistics (Fig 6, Fig 7) show that there are large biases in both midlatitudes and tropics and the RMS and anomaly correlations are noticably worse than the other models.

At this stage we are still testing the V-D SL model, so we can not rule out the possibility of coding errors. However, assuming the coding is correct, the reasons for these model deficiencies would then lie with the formulation. Compared to the U-V scheme there are clearly more and larger nonlinear terms which are calculated explicitly in the V-D scheme, and in general these terms will contribute to the numerical stability limitation. The accuracy of the semi-Lagrangian advection scheme could be being influenced by the accuracy of the interpolation, which in the V-D scheme is performed on differentiated quantites which are less smooth than the fields being interpolated in the U-V scheme.

In order to isolate whether the treatment of one or other of vorticity and divergence is making the larger difference between the U-V and V-D schemes we have modified the code to take the vorticity contribution each time step from the V-D scheme and divergence from the U-V scheme (labelled VD-VOR) and vice versa (VD-DIV). Both these hybrid schemes have been run with both 20 min and 9 min time steps on the 1 February case and even with the larger time step they both run successfully to 5 days. Comparing the forecasts with the U-V SL and V-D SL models shows that the the treatment of vorticity is much more significant than divergence — the VD-DIV hybrid which uses the U-V scheme for vorticity is closer to the U-V SL model, and the VD-VOR hybrid is closer to the V-D SL model (Fig 8). Note that the formulation of the VD-VOR hybrid has similarities with the potential vorticity semi-Lagrangian model of Bates et al. (1995) which advects potential vorticity using the scalar potential vorticity equation and obtains divergence from a semi-Lagrangian scheme for the vector momentum equations.

Another type of hybrid calculation was also made as a precursor to implementatio n of the V-D SL scheme to see whether the Eulerian divergence equation was contributing to the CFL time step limitation in the same way as the other fields. Whilst vorticity, temperature and moisture are all clearly advected by the flow field it is not so clear whether this is as much the case for divergence, especially since the flux form of the divergence equations has no explicit $\nabla.(\mathbf{u}\delta)$ term in it like the other fields. The hybrid code picks up the divergence Q term from the Eulerian scheme and the other Q fields from the U-V SL scheme in spectral space immediately before the implicit part of the time stepping calculation. The results show that the stability characteristics are essentially the same as the Eulerian model, since with a 20 min time step the model becomes unstable after 8 hours. Otherwise, with the smaller step, the results are comparable to the ordinary U-V SL scheme.

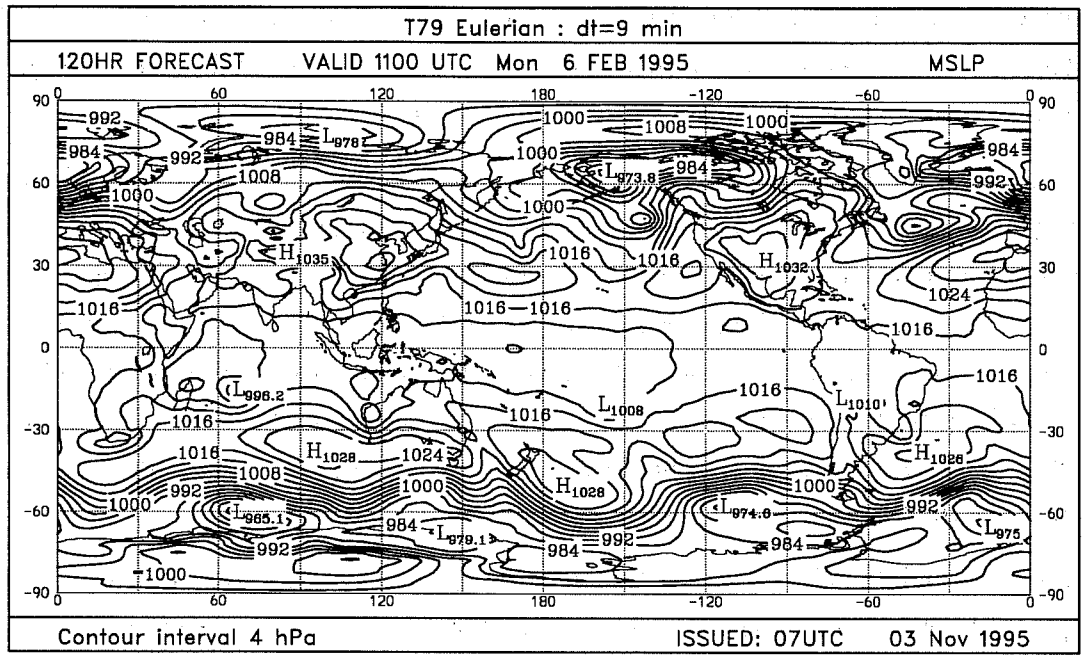
T79 Eulerian : dt=9 min
120HR FORECAST VALID 1100 UTC Mon 6 FEB 1995 MSLP
Contour interval 4 hPa
ISSUED: 07UTC 03 Nov 1995

Fig 5a.

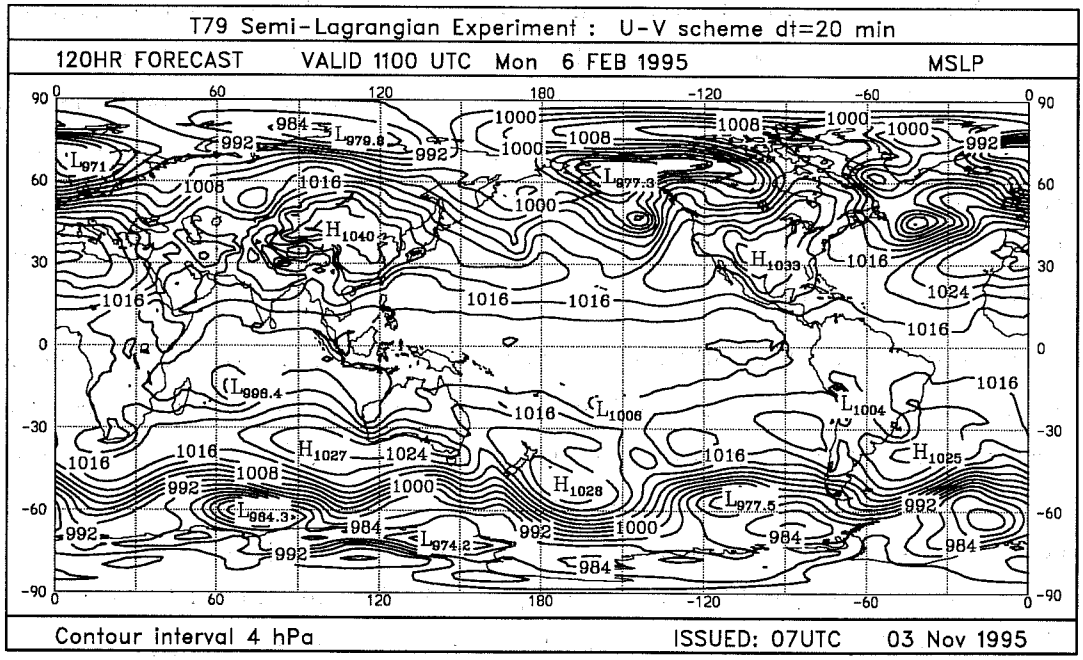
T79 Semi-Lagrangian Experiment : U-V scheme dt=20 min
120HR FORECAST VALID 1100 UTC Mon 6 FEB 1995 MSLP
Contour interval 4 hPa
ISSUED: 07UTC 03 Nov 1995

Fig 5b.

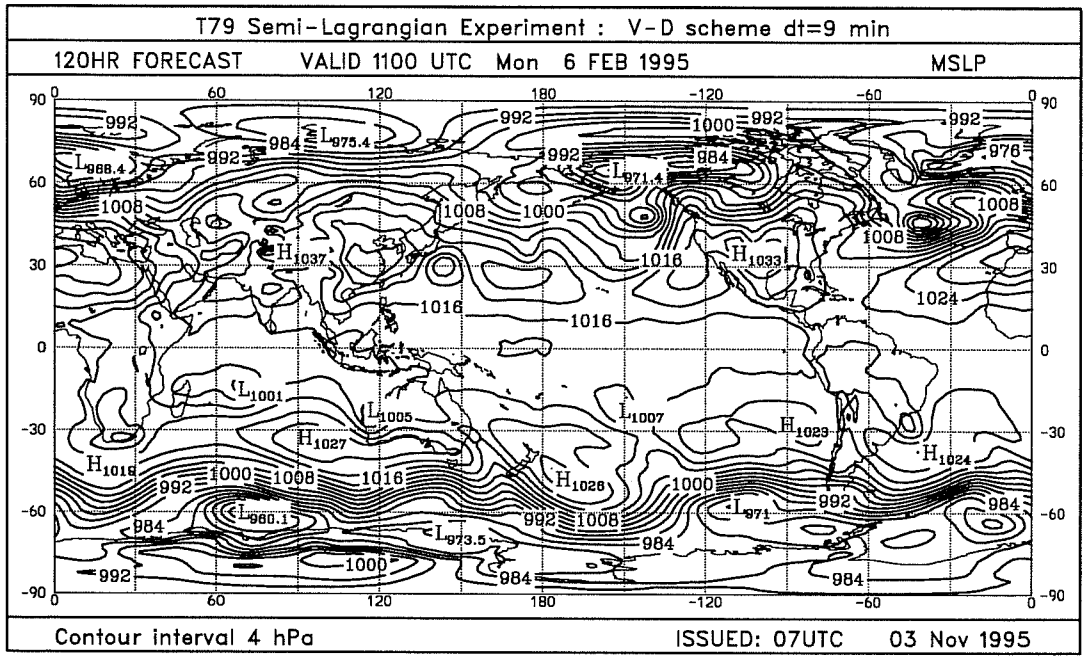
T79 Semi-Lagrangian Experiment : V-D scheme dt=9 min
120HR FORECAST VALID 1100 UTC Mon 6 FEB 1995 MSLP
Contour interval 4 hPa
ISSUED: 07UTC 03 Nov 1995

Fig 5c.

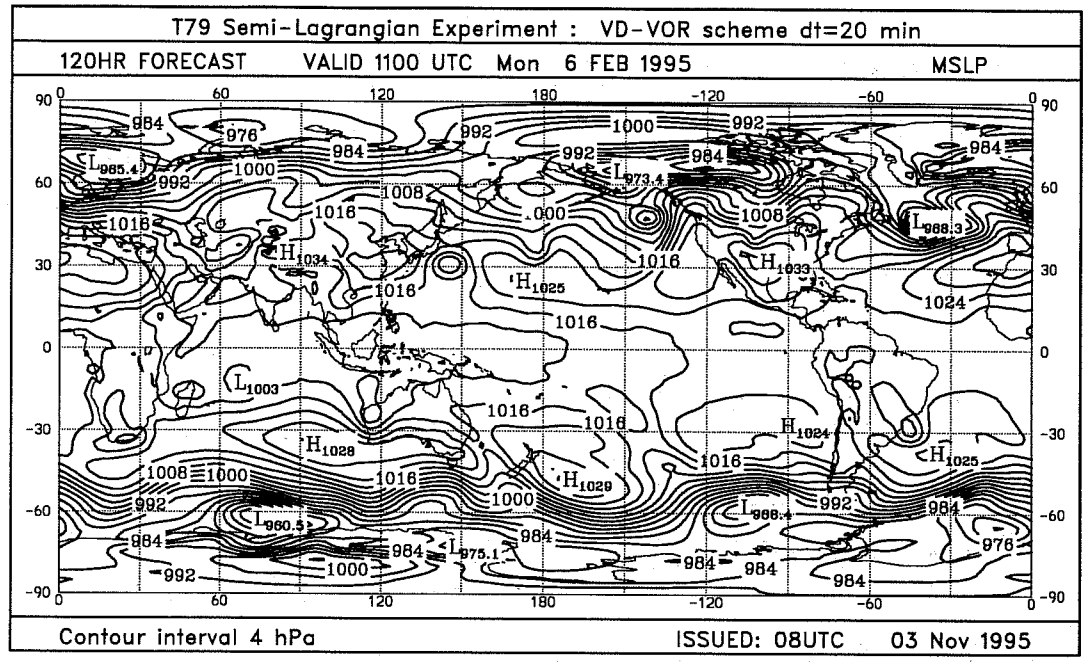
T79 Semi-Lagrangian Experiment : VD-VOR scheme dt=20 min
120HR FORECAST VALID 1100 UTC Mon 6 FEB 1995 MSLP
Contour interval 4 hPa
ISSUED: 08UTC 03 Nov 1995

Fig 5d.

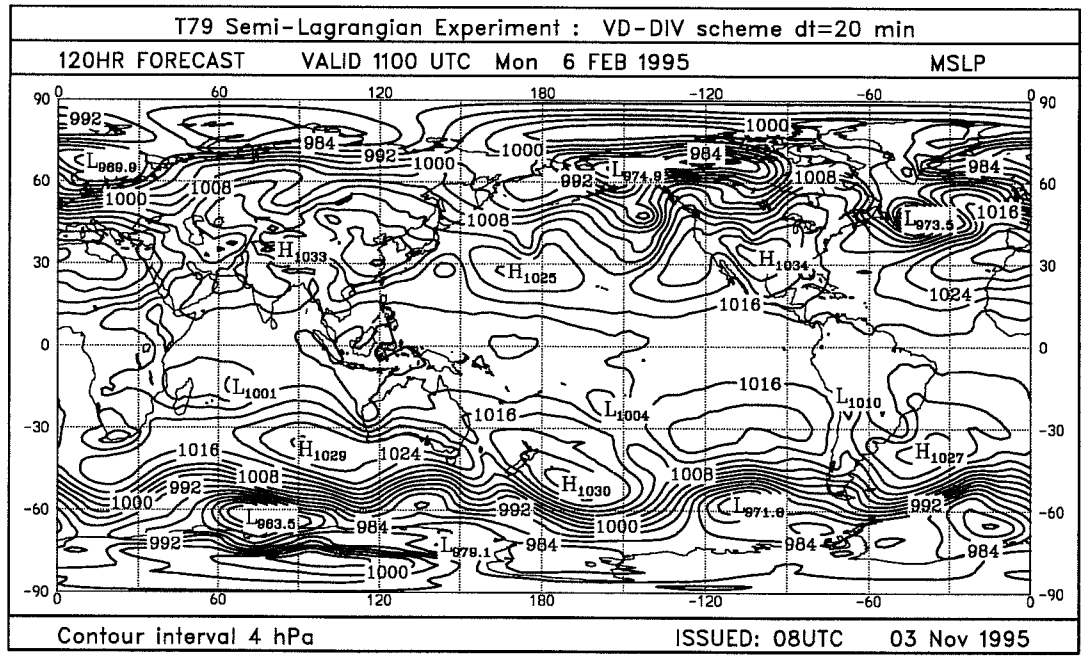
T79 Semi-Lagrangian Experiment : VD-DIV scheme dt=20 min
120HR FORECAST VALID 1100 UTC Mon 6 FEB 1995 MSLP
Contour interval 4 hPa
ISSUED: 08UTC 03 Nov 1995

Fig 5e.

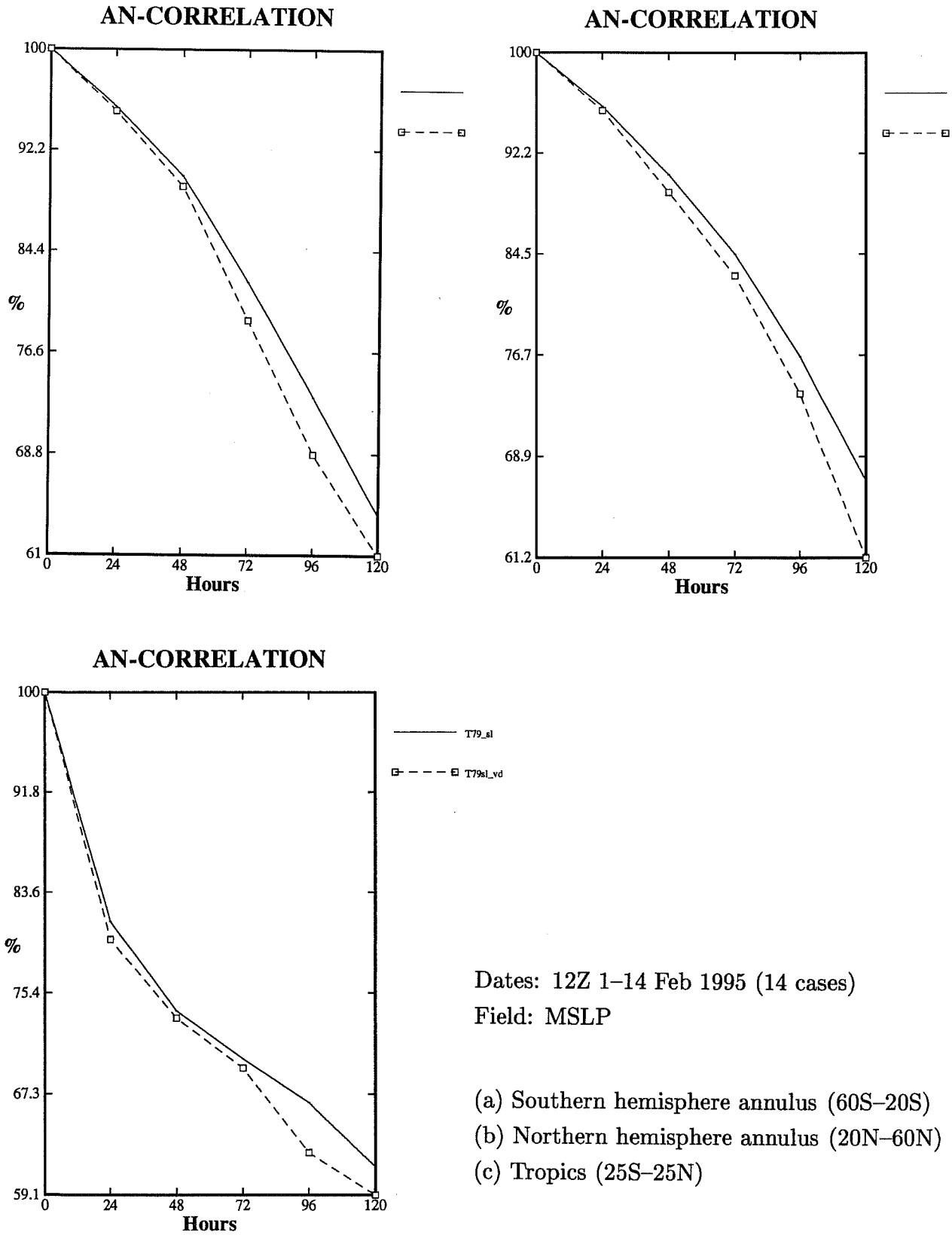

Dates: 12Z 1–14 Feb 1995 (14 cases)
Field: MSLP

(a) Southern hemisphere annulus (60S–20S)
(b) Northern hemisphere annulus (20N–60N)
(c) Tropics (25S–25N)

Fig 6. [**T79_sl**] U-V Semi-Lagrangian T79 vs [**T79_sl_vd**] V-D Semi-Lagrangian T79.

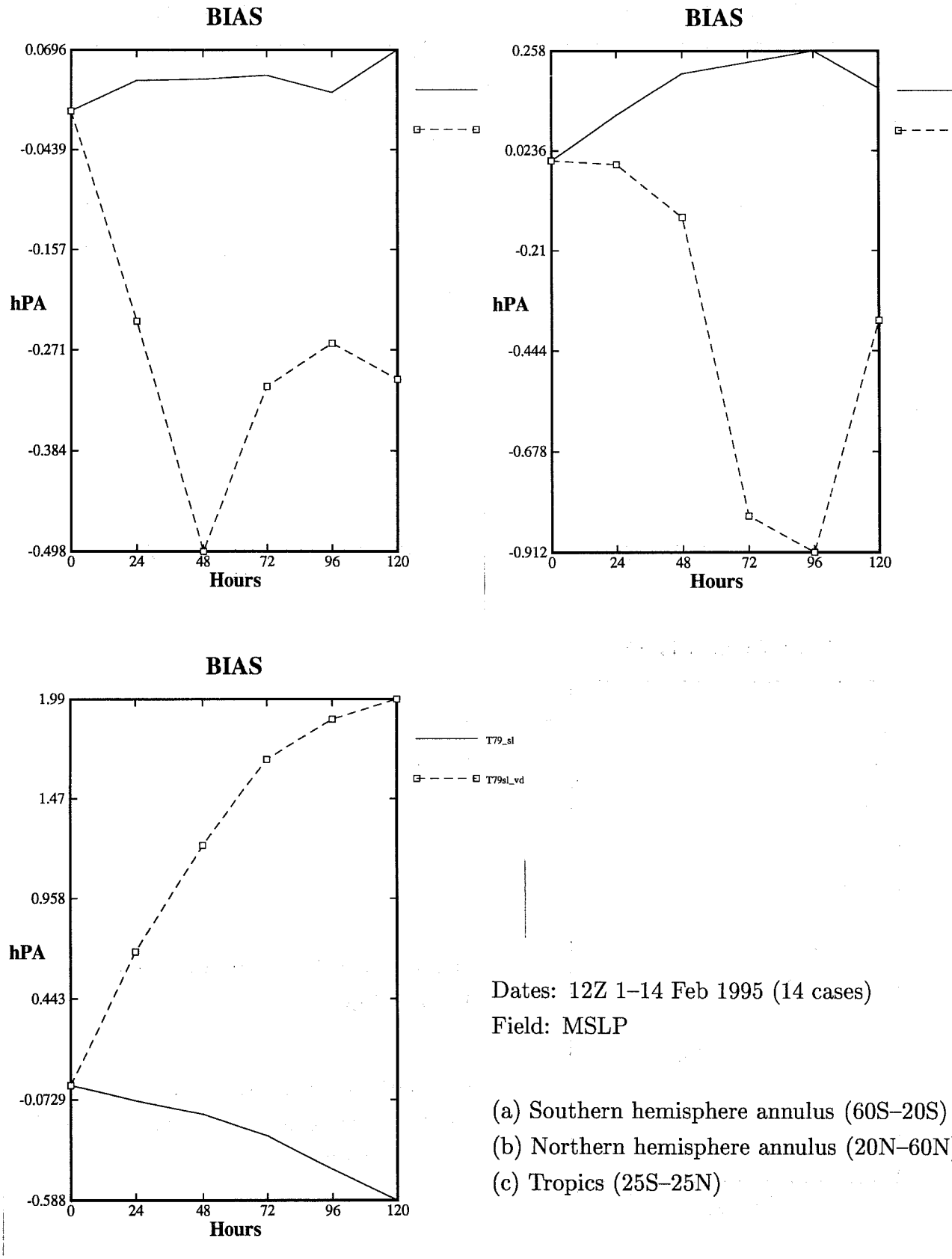

Dates: 12Z 1–14 Feb 1995 (14 cases)
Field: MSLP

(a) Southern hemisphere annulus (60S–20S)
(b) Northern hemisphere annulus (20N–60N)
(c) Tropics (25S–25N)

Fig 7. [**T79_sl**] U-V Semi-Lagrangian T79 vs [**T79_sl_vd**] V-D Semi-Lagrangian T79.

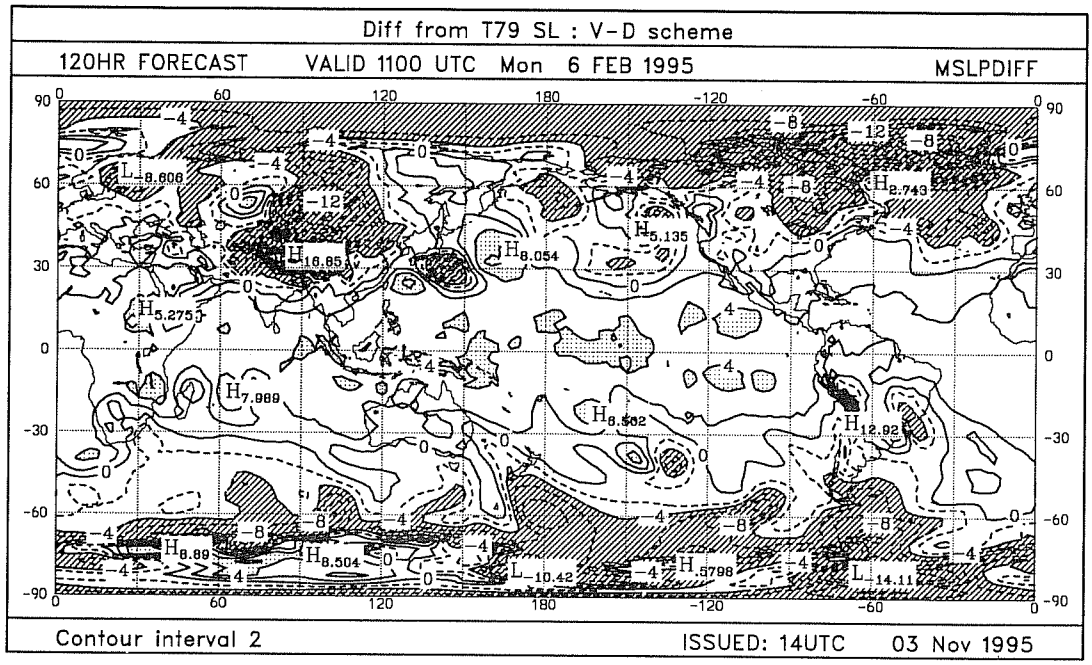

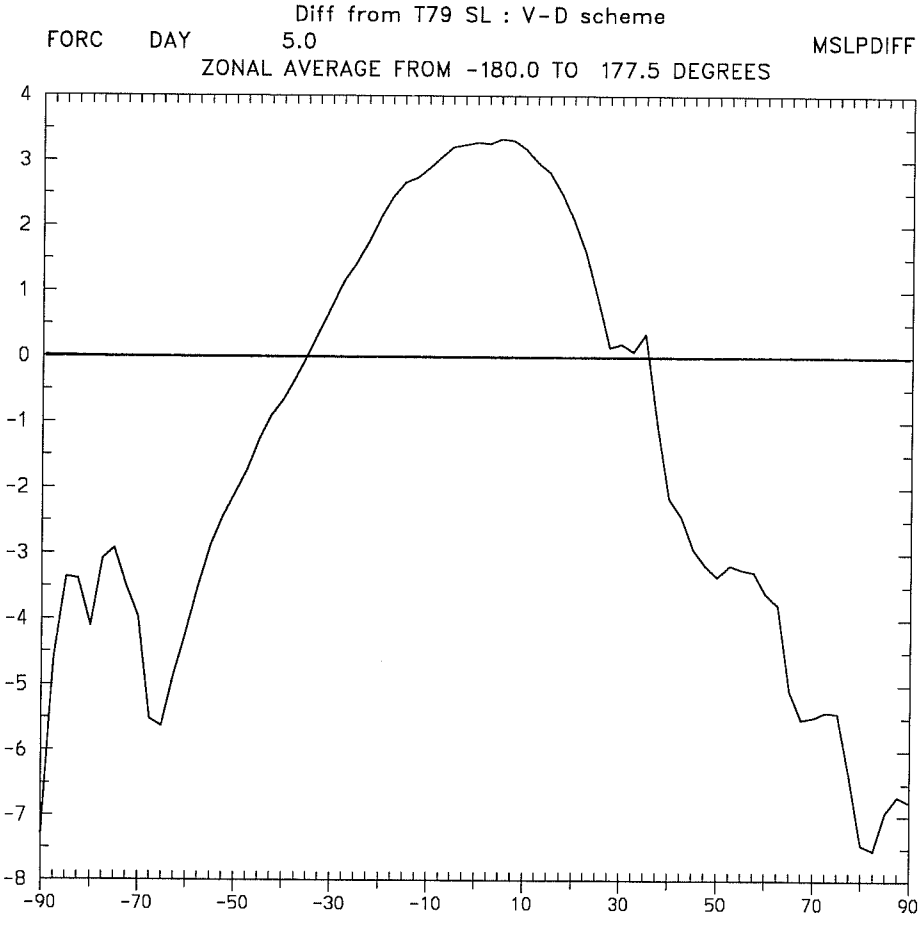

Fig 8a. Difference between T79 V-D and T79 U-V semi-Lagrangian forecasts.

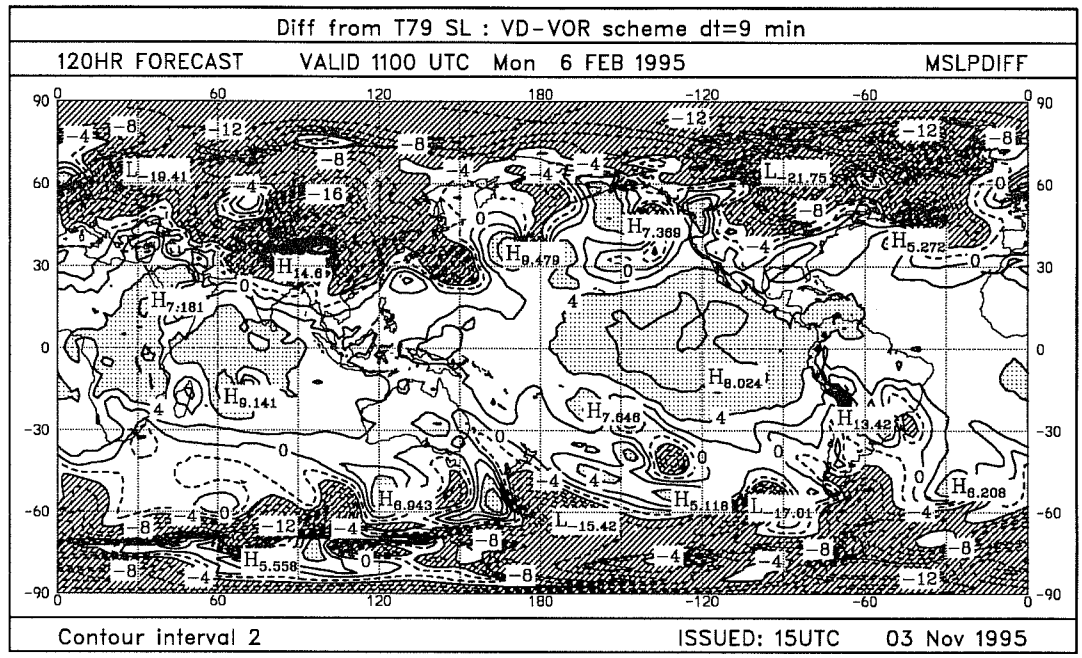

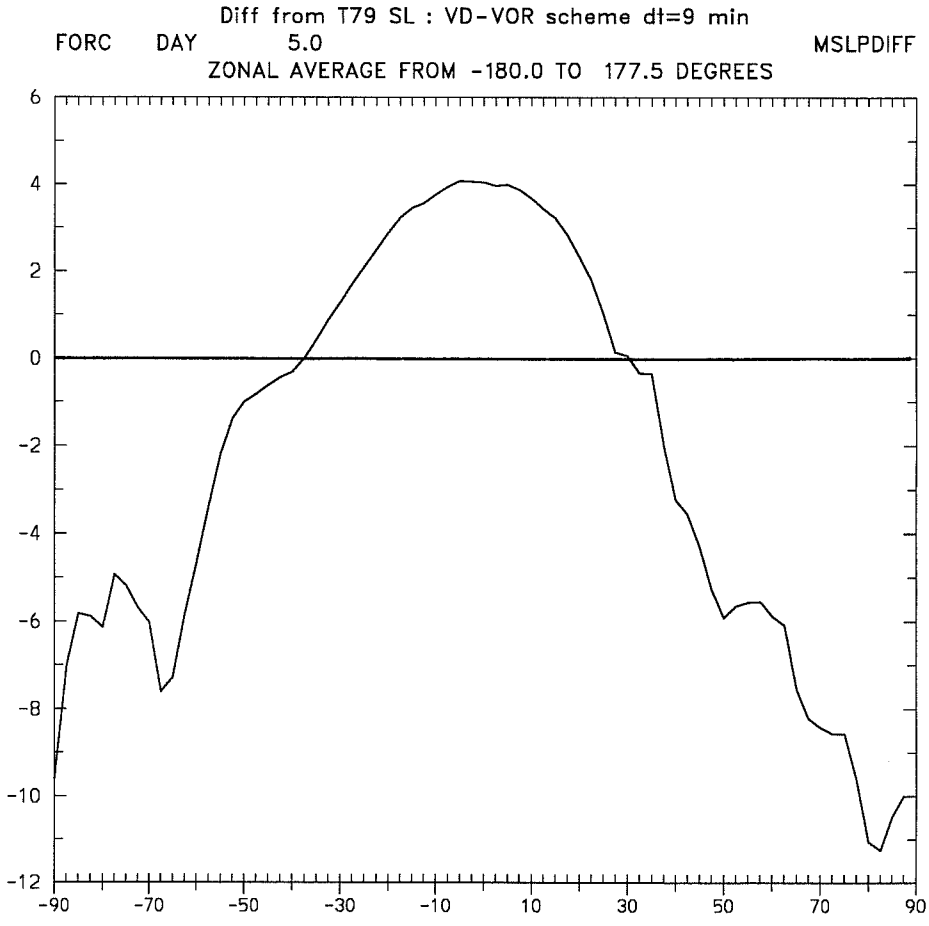

Fig 8b. Difference between T79 VD-VOR and T79 U-V semi-Lagrangian forecasts.

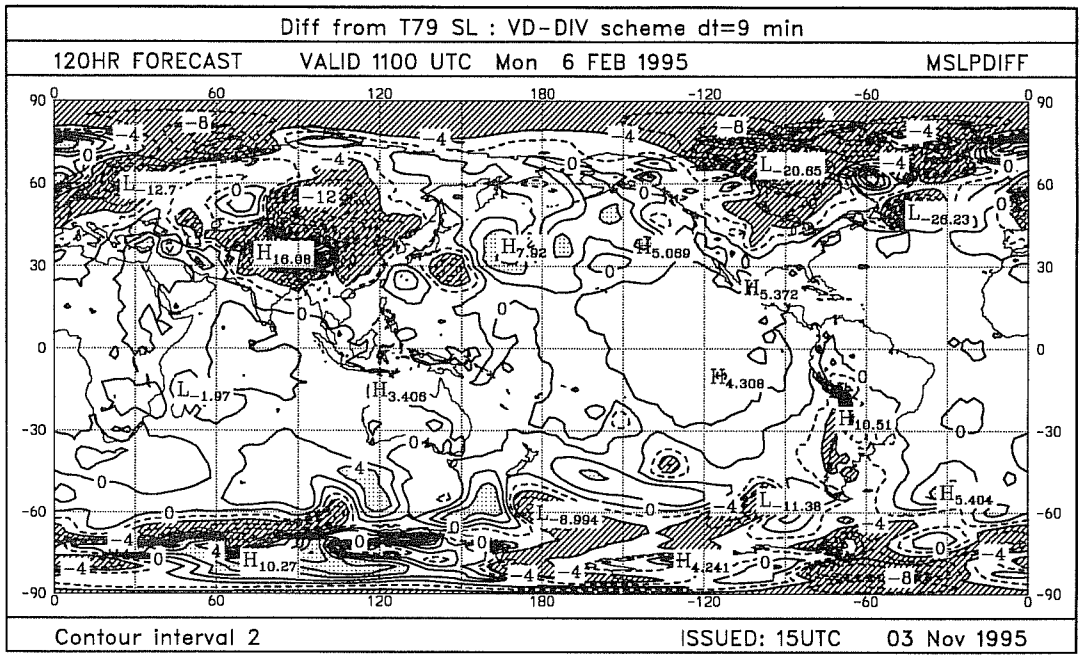

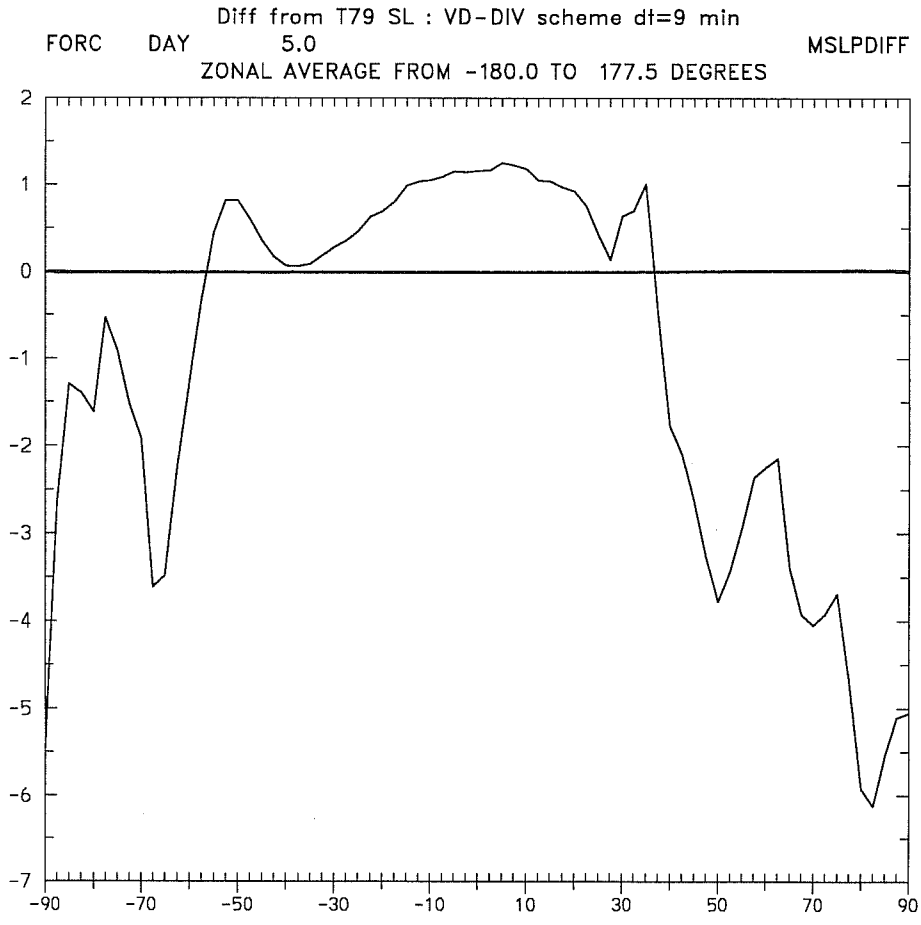

Fig 8c. Difference between T79 VD-DIV and T79 U-V semi-Lagrangian forecasts.

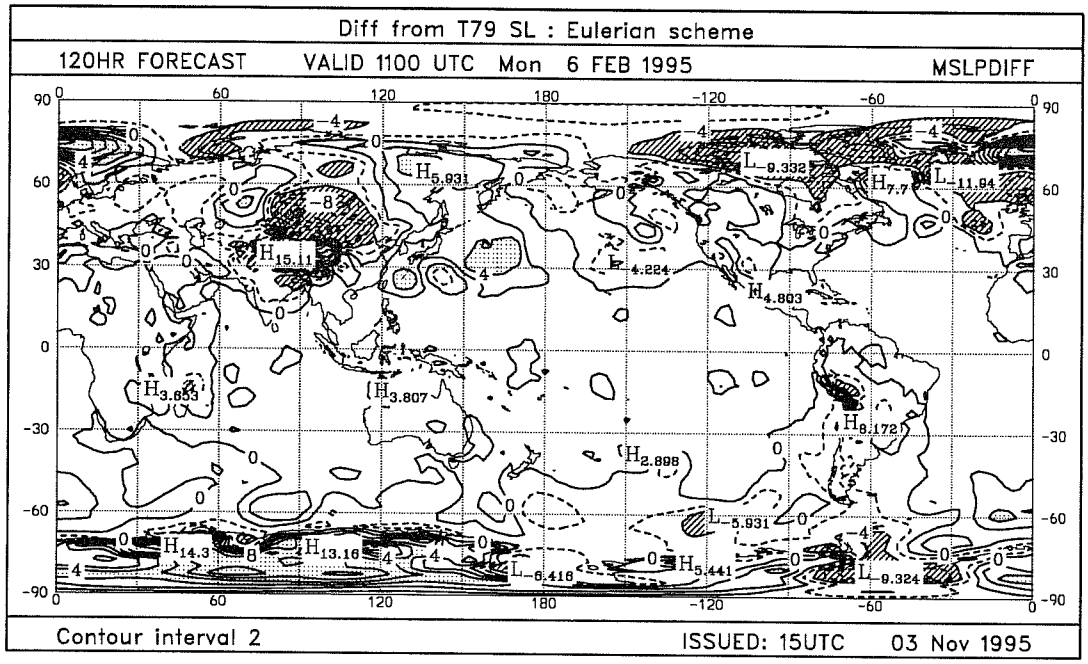

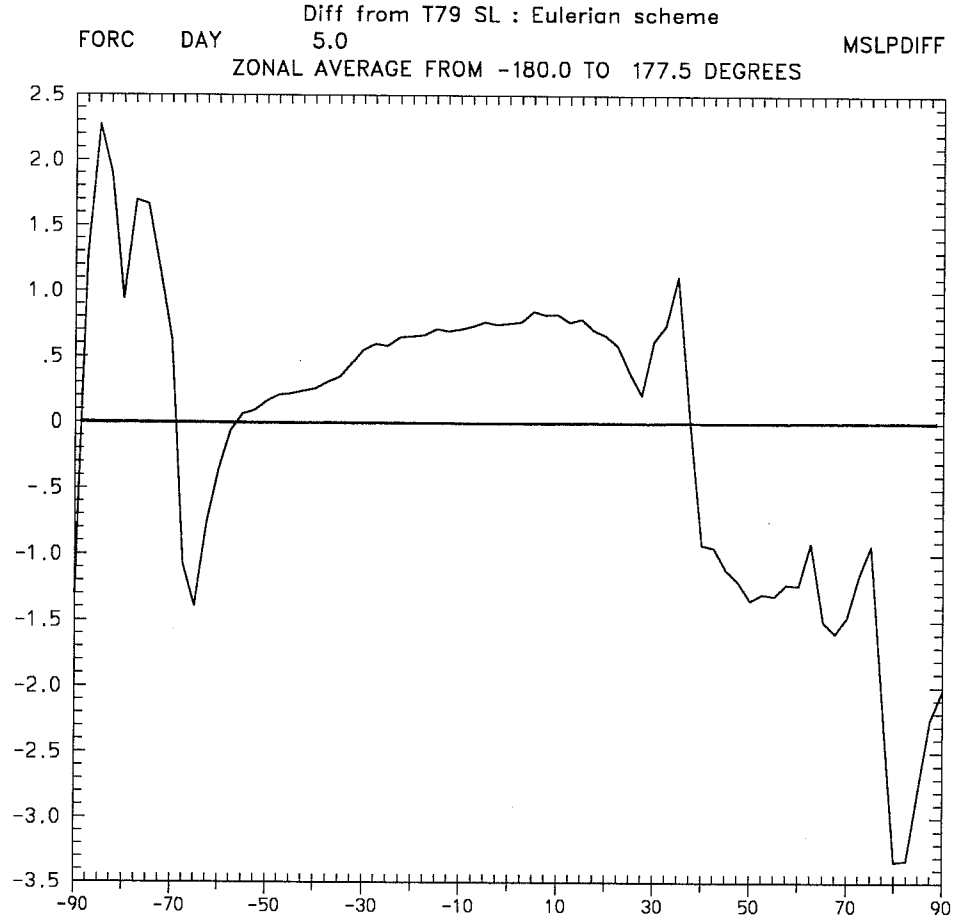

Fig 8d. Difference between T79 Eulerian and T79 U-V semi-Lagrangian forecasts.

REFERENCES

Bates, J.R., Y. Li, A. Brandt, S.F. McCormick and J. Ruge, 1995: A global shallow water numerical model based on the semi-Lagrangian advection of potential vorticity. *Quart. J. Roy. Meteor. Soc.*, in press.

Bourke, W., 1972: An efficient one-level primitive-equation spectral model. *Mon. Wea. Rev.*, **100**, 683-698.

Bourke, W., 1974: A multi-level spectral model. I. Formulation and hemispheric integrations. *Mon. Wea. Rev.*, **102**, 687-701.

Bourke, W., B. McAvaney, K. Puri and R. Thurling, 1977: *Global modelling of atmospheric flow by spectral methods. Methods in Computational Physics, Vol. 17*, ed. J. Chang, Academic Press, 267-324.

Bourke, W., 1988: Spectral methods in global climate and weather prediction models. *Physically-based modelling and simmulation of climate and climate change.*, ed. M.E. Schlesinger, Kluwer Academic Publishers, Part I, 169-220.

Bourke, W., T. Hart, P. Steinle, R. Seaman, G. Embery, M. Naughton and L. Rikus, 1995: Evolution of the Bureau of Meteorology's Global Assimilation and Prediction system. Part 2: resolution enhancements and case studies. *Aust. Met. Mag.*, **44**, 19-40.

Courtier, P., and M. Naughton, 1994: A pole problem in the reduced Gaussian grid. *Quart. J. Roy. Meteor. Soc.*, **120**, 1389-1407.

Dent, D., 1992: Modelling and parallelism, in "Modelling Weather and Climate"", BMRC Research Report No. 33, 165-178 (available from BMRC, Melbourne, Australia).

Hortal, M., and A.J. Simmons, 1991: Use of reduced Gaussian grids in spectral models. *Mon. Wea. Rev.*, **119**, 1057- 1074.

Ritchie, H., 1988: Application of the semi-Lagrangian method to a spectral model of the shallow water equations. *Mon. Wea. Rev.*, **116**, 1587-1598.

Ritchie, H., 1991: Application of the semi-Lagrangian method to a multilevel spectral primitive-equations model. *Q. J. R. Met. Soc.*, **117**, 91-106.

Ritchie, H., and C. Beaudoin, 1994: Approximations and sensitivity experiments with a baroclinic semi-Lagrangian spectral model. Mon. Wea. Rev., 122, 2391-2399.

Ritchie, H., C. Temperton, A. Simmons, M. Hortal, T. Davies, D. Dent and M. Hamrud, 1995: Implementation of the semi-Lagrangian method in a high resolution version of the ECMWF forecast model. *Mon. Wea. Rev.*, **123**, 489-514.

Tanguay, M., E. Yakimiw, H. Ritchie, and A. Robert, 1992: Advantages of spatial averaging in semi-Lagrangian schemes. *Mon. Wea. Rev.*, **120**, 113-123.